TEMPERATURE WAVES IN SRF RESEARCH*

A. Ganshin[#], R.G. Eichhorn, D. Hartill, G.H. Hoffstaetter, X. Mi, E. Smith and N. Valles, Cornell Laboratory for Accelerator-based Sciences and Education, Newman Laboratory, Ithaca, New York, 14853 U.S.A

Abstract

The localization of the quench spot on the surface of a superconducting elliptical-cell radio-frequency cavity operating at high field gradients is a goal of modern SRF diagnostics. We report here an efficient method of the visualization of quench position by detection of the superfluid helium second sound waves propagating in superfluid helium. Results characterizing defect location with second sound waves, oscillating superleak transducer (OST) detection and newly developed software will be presented.

CAVITY DEFECTS AND METHODS OF THE DETERMINATION

Until recently there was only one reliable technique to diagnose energy losses during cavity operation and find possible defects responsible for the quench - temperature mapping. Temperature mapping requires hundreds to thousands of fixed thermometers attached to the culprit cavity to identify the approximate quench location. After that measurement with many localized thermometers is necessary to zoom in on the quench spot. Also, for reliable sensor measurement, advanced and expensive electronics must be used. The situation becomes even more complicated when the temperature map system must be used for defect localization in multi cell cavities such as seven cell ERL and nine cell ILC cavities. Optical inspection cannot always provide unambiguous interpretation of quench caused defects [1].

A powerful alternative technique to resistance thermometry is the use of 2nd sound in superfluid helium to image the heat transfer from the resonator to the superfluid helium bath. By testing a superconducting resonator in a superfluid helium bath it is possible to observe the second-sound temperature and entropy waves driven by the conversion of stored RF energy to thermal energy at a defect. By measuring the time-of-arrival of the second sound wave at three or more detectors which form a basis for the resonator's three dimensional coordinate system, the defect location can be unambiguously determined. For our research we used the unique property of superfluid helium, its ability to support propagation of temperature or entropy waves, called second sound. The velocity of the second sound is an order of magnitude less then the velocity of the

"traditional" density waves and near the cavity operational temperature at 2 K is 16 m/s. This give us the possibility to get adequate time/place resolution of the quench spot (1cm spatially for 0.5 msec timing).

EXPERIMENTAL TECHNIQUE AND ELECTRONICS

For the detection of the second sound waves we are using the concept of the oscillating superleak transducer (OST) immersed in superfluid helium [2]. A typical OST arrangement uses 8 to 16 transducers evenly distributed around the cavity. It is convenient to record all second sound traces by a 16 channel Data Acquisition Card, we used model DT9834; the number of channels (OST's) can be easily extended by adding another card via USB port. For the operation of the DAQ card the level of the signal should be on order of one volt magnitude. For this purpose we designed a multistage low noise preamplifier, electrical circuit shown in figure 1. The electrode behind the porous membrane is biased at 70 V, which is current limited by a large resistor to avoid heating in the cryostat in the event of a short-circuit through the diaphragm.
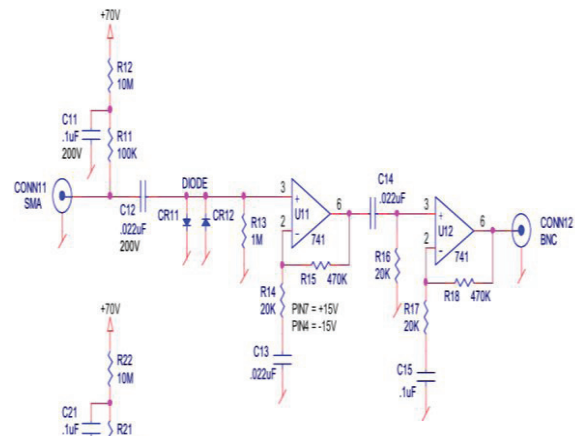

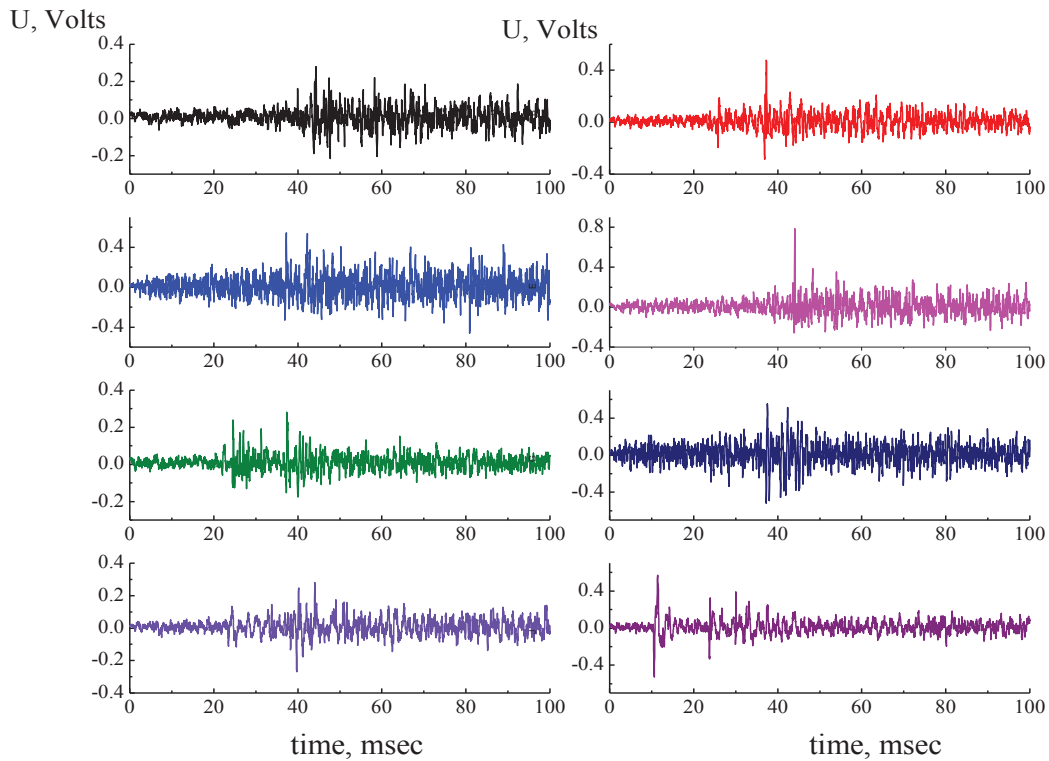Figure 1: Electrical diagram of the preamplifier circuit.

Figure 2: Second sound signals detected by multichannel DAQ card.

Figure 2 demonstrates second sound traces from a quench event of a nine cell cavity at a helium bath temperature of 2.005 K where t=0 corresponds to the quench event as determined by rf transmitted power measurement in the cavity. For calculation of the quench location we created a Matlab code, that can model the cavity according to drawings specification, input the temperature at which the data was collected, models the OST positions and their geometry, calculates and save the distances between pairs of vertices which define the cavity as well as calculate and save the distances between the vertices which define the cavity and the OSTs.

The current code allows us to evaluate timing data and statistical error and to input geometrical data and systematic error. There is an option to load previously calculated and saved cavities (with vertex pair calculations) and OSTs (with vertex-OST calculations). It is possible to calculate the quench location using one of two different methods, choose specific OSTs to use, and display the error.

Geometries of standard Tesla cavity and re-entrant cavity can be selected from a list. Once the vertex-pair calculations are completed, they can be used to find the shortest distance from each vertex to each OST by selecting option "complete method of calculation" inside software. This takes a significant amount of time, so the alternative method "Direct Lines of Sight Only" can be picked from the drop down menu.

This method only takes into account direct lines of sight between vertices and OSTs (draw a line straight from a vertex to an OST. If that line intersects the cavity at any location, that OST will not be used when evaluating the likelihood that this vertex is the quench location.) The program will only consider vertices that have direct lines of sight to at least three OSTs. Often, this means that only points near the equators will be considered as quench locations. This method avoids the need for extensive vertex-pair calculations, but is not as complete as the original method.

Considering a single vertex on a cavity the program evaluates the shortest distance between the vertex and each OST. Call these distances $d_n(\alpha,\beta)$. The values of (α,β) simply pick a specific vertex. The velocity of the second sound wave is determined from the helium bath temperature. The arrival time of second sound t_n from the quench spot recorded by each OST and errors σ_n associated with these times is known. N is the total number of OSTs, and n corresponds to a specific OST. The program finds the vertex (α,β) and variable parameter, γ, that minimize the sum,

$$\chi^2 = \sum_n^N \left\{ \frac{[t_n + \gamma - \frac{d_n(\alpha,\beta)}{v}]}{\sigma^2} \right\}^2 \tag{1}$$

The quench vertex, values of gamma, velocity, average χ^2, and errors in alpha, beta and gamma appear in the title above the graph after the calculations have taken place, as it is shown in figure 3.

04 Measurement techniques
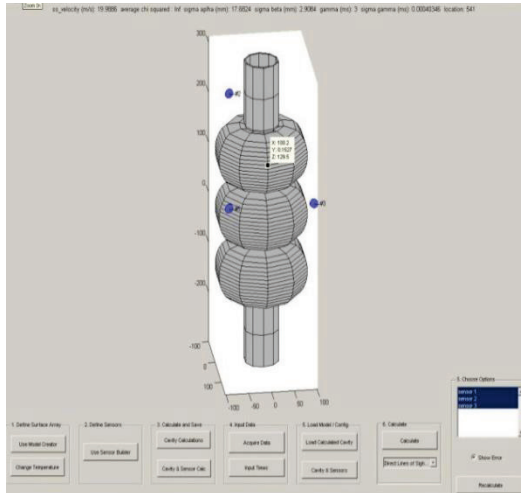
T. T-mapping and Second Sound

Figure 3: Three dimensional picture of SRF cavity with localized quench spot using MATLAB code.

MEASUREMENTS OF PROPAGATION OF SECOND SOUND WAVES IN A TEST DEWAR

Experimentally we were able to determine how the geometry of the Dewar affected the sound of the second sound wave received. We used various thicknesses of aluminium and G10 and drilled holes in some of them.

Experimental Set Up

For understanding the propagation of second sound waves in restricted geometry where number of obstacles play a role we performed a number of modelling experiments in a small Dewar.

The heater to excite the second sound waves was glued by Stycast 2850FT epoxy to an aluminium post which was attached to a non-conductive G-10 plate, as shown in Figure 4a. There is a separation of 12 mm between the heater and the post with three OST's for the detection of arrival second sound waves which is also anchored to the G10 plate. When testing we need to make sure that the helium level in the Dewer is high enough. In order to do this we use quartz tuning forks [3].

During our experiments we made four sets of tests.

1. Propagation of the second sound in an open geometry, without any barriers between heater and detectors.

2. 3 mm aluminum plate and G-10 non-conductive 12 mm plate was placed at an intermediate distance between heater and detectors

3. An aluminum plate (thickness 0.5mm) was moved close to the heaters post. Three heaters

were glued to the G-10 post. Two 3mm and one 6mm holes were drilled directly opposite the heaters in the same sight line as the OST's detectors, figure 4b.
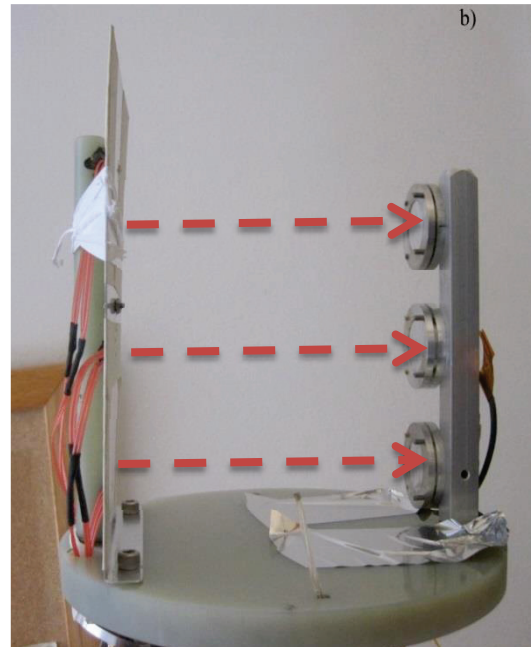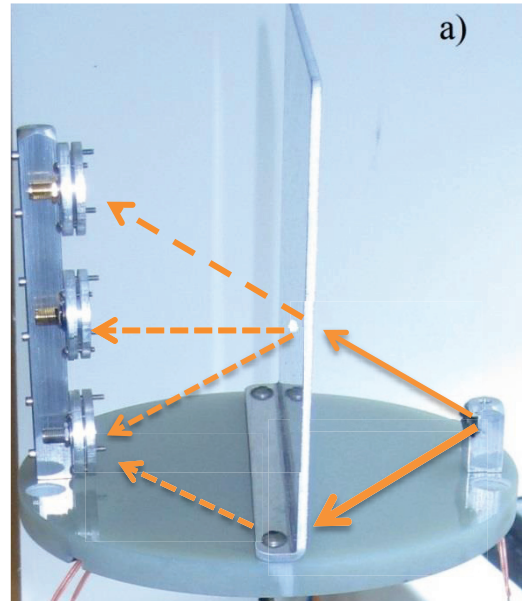

Figure 4: Experimental set up a) top - with the solid metal screen in the middle of the cell, later with 6mm hole, b) bottom - screen with drilled holes near the heaters.
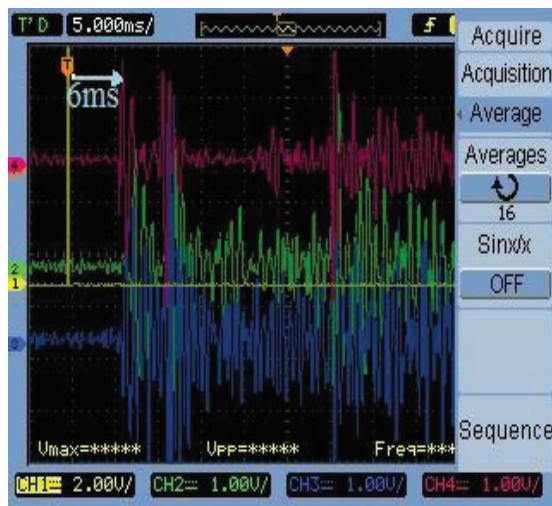
Figure 5: Detection of second sound waves in open geometry.

Figure 6: Results from 3mm thick Al plate.

Figure 5 shows the propagation of second sound waves in open geometry launched from the heater. The first arrived signal with a travel time 6ms corresponding to the shortest path (~ 12 mm) from the heater to the OST, where the velocity of second sound at 1.65 K is 20.36 m/sec [4]. The other two signals have been reflected from walls and the top plate and have therefore taken longer to be received.

Interestingly the reflected signal has larger amplitudes compared to the direct one. This is a result of the focusing of reflected temperature waves from the curved walls of the Dewar. The heat flux during the pulse was 17 W/cm^2.

Next we illustrate the case when the direct path from the heater (with the same heat flux) to the OST was covered by a non-transparent screen (figure 4a). Three sets of data are shown in Figure 6. The strongly attenuated signal was detected by three OST's. The earliest arrival time 6ms was recorded by OST 1 due to the second sound penetrating through 0.5 mm gap between top plate and screen. The other OST's start to detect signals with later arriving time, around ~0.01 sec, due to being reflected off of the bottom of the Dewar, bypassing the barrier. During the experiments we replaced 3mm Aluminium screen with 0.5mm and 12 mm G-10, no visible differences in waves propagation have been observed.

Next we studied the traces recorded by OST's for two different cases. During case (b) the screen was moved closer to the heater and the top gap was removed.
a. The aluminum plate was placed in the middle of the cell figure 5a, the heat source was 40 mm away from the 6mm hole
b. The screen was shifted towards the pile with heaters, the distance between the heater and source was less than half a millimeter.
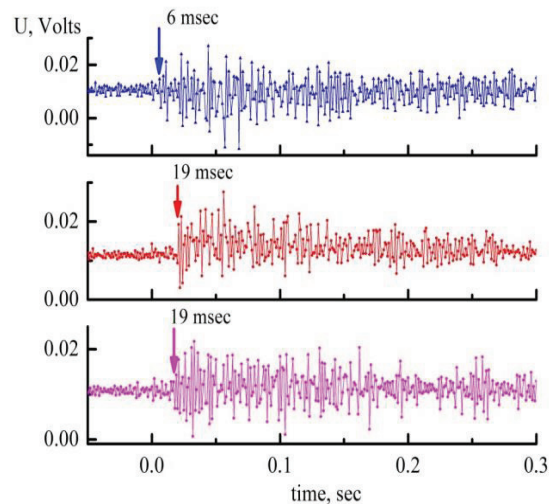
Figure 7 illustrate case a) hole in the plate located in the middle of the cell.
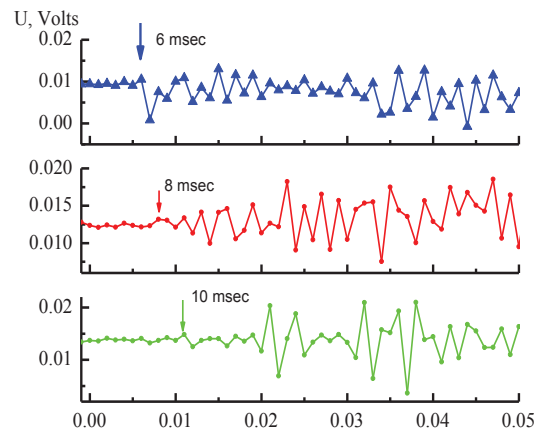

Figure 7: Plate with 6mm hole in metal plate 40mm apart from the heater.

If one compares the signal in figure 6 with the signal in the open geometry (figure 5) we clearly see the strong attenuation of the amplitude by almost a factor of 100. Also only the OST lying on the same straight line heater - hole – detector correctly records the propagation time, even the nearest OST's 20 cm apart detect a weak signal so small it masks the onset time.

For figure 8, even ~1 mm separation between heater and hole decreases heat flux propagated through the hole and lead to the suppression of the detected signals. Also there is extra amplitude decrease of the detected signal by OST's shifted from line of sight. The time propagation of second sound waves for all detected signal correctly corresponds the path between source and detector and velocity of second sound.
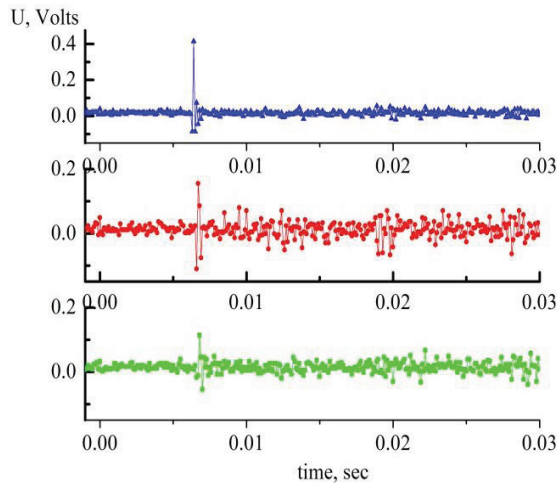
Figure 8: Heat source near (less than 1mm separation) to the 3mm hole.

CONCLUSIONS

In this paper we continue investigation of the technique developed at Cornell of quench localization in superconducting niobium cavities during RF tests by detection of temperature (second sound) waves. We describe hardware such as a low noise preamplifier and a DAQ card and a newly developed software for in-situ determination of quench location. We made a number of modelling tests where the distance between heat source and detectors as well as propagation pattern were well known. It was shown that only direct line-of-sight between OSTs and heater give consistently correct determination of propagation time or heater location. Potentially an increase of the number of OST's may be required for reliable localization of the quenching spot. Currently developed technique allows us to do it with minimum efforts by increasing number of channels or DAQ cards.

REFERENCES

[1] S. Posen, N. R. A. Valles, M. Liepe, QUENCH STUDIES IN LARGE AND FINE GRAIN Nb CAVITIES, Proceedings of SRF2011, Chicago, IL USA.

[2] R. Williams, S.E.A. Beaver, J.C. Fraser, R.S. Kagiwada and I. Rudnick, Physics Letters 29A, 279 (1969).

[3] A. N. Ganshin, X . Mi, E. N. Smith and G. H. Hoffstaetter, Use of quartz tuning forks for sensitive, *in-situ* measurements of helium properties during SRF cavity tests , 2013 JINST **8** P04007 doi:10.1088/1748-0221/8/04/P04007.

[4] Russell J. Donnelly and Carlo F. Barenghi, The Observed Properties of Liquid Helium at the Saturated Vapor Pressure, http://pages.uoregon.edu/rjd/vapor1.htm.